ELECTRONIC SUPPORTING INFORMATION

Bicomponent hydrogen-bonded nanostructures formed by two complementary molecular Landers on Au(111)

N. Kalashnyk,[a] M. Yu,[a] R. Barattin,[b] Y. Benjalal,[c] M. Hliwa,[bc] C. Joachim,[b] E. Lægsgaard,[a] F. Besenbacher,[a] A. Gourdon,[b] X. Bouju*[b] and T. R. Linderoth*[a]

[a] Interdisciplinary Nanoscience Center (iNANO) and Department of Physics and Astronomy, Aarhus University, Aarhus 8000, Denmark.
E-mail: trolle@inano.au.dk
[b] Nanosciences group, CEMES-CNRS, UPR 8011, Bât. picoLab, BP 94347, F-31055 Toulouse, France.
E-mail : xavier.bouju@cemes.fr
[c] Faculté des Sciences Ben M'Sik, Université Hassan II-Mohammédia, Casablanca BP 7955, Morocco.

Methods - the STM experiments were performed in an ultrahigh vacuum (UHV) chamber (base pressure in the low 10^{-10} mbar region) equipped with standard facilities for sample preparation as well as a non-commercial version of the variable-temperature Aarhus scanning tunneling microscope (STM). Cleaning of the single-crystal Au(111) surface was achieved by repeated cycles of Ar+ ion sputtering at 1.5 keV for 20 min followed by sample annealing at 850 K for 10 min, resulting in a well-ordered herringbone reconstruction. The cleaned Au(111) substrate was maintained at a temperature of 220 K during deposition of molecules. The Lander molecules were synthesized by the methods described elsewhere. Thorough degassing of molecular powders was performed prior to evaporation. Lander DAT and DCI molecules were thermally sublimated from separate glass crucibles resistively heated to 543 and 700 K, respectively. The codeposition of these molecules was followed by immediate annealing at 400 K for 10 min. Temperatures were monitored with NiCr/Ni thermocouple pairs. The molecular coverage of the surface was controlled by evaporation times in the range 2-5 min and 10-20 min for Lander DAT and Lander DCI, respectively. STM imaging occurred at sample temperatures ranging from 110–160 K in the constant current mode ($I_T \sim 0.26$ nA). Bias voltages ($U_T \sim -1.25$ V) are given with respect to the sample. Attentive survey of the surface did not disclose any hint for molecular fragments. The STM images were calibrated from images of the clean Au(111) surface.

Methods - the calculations of STM images (Fig. S1) were performed using extended Hückel molecular orbital-elastic-scattering quantum chemistry (EHMO-ESQC) method[S1,S2] after having

relaxed the molecule on the surface with the molecular mechanics MM4(2003) code.[S3,S4] The coupling of molecular mechanics to ESQC calculations has already been applied for Lander type molecules with success.[S5] The MM4 code is based on a force field including standard potential functions to describe internal interaction and long-range intermolecular interactions as well. In particular for these later, van der Waals and H-bonding are considered. The accuracy of the calculations lies on the pertinent choice of interaction parameters. The MM4 force field has already demonstrated its accuracy through the various experiment/calculation comparisons found in the literature. In terms of precision, one may estimate the energies at ± 10 meV.

Once the interacting system is fully relaxed, the configuration is frozen and the vdW and H-bonding are switched on/off to calculate the respective contributions of these two interactions. The substrate is composed of four gold layers without any reconstruction.

Table S1 Calculated total energy comprising the hydrogen bonding (HB) and van der Waals interaction (vdW) for 2-D and 1-D structures formed by molecular Landers on the terraces and steps.

	2D structure on terrace	1D chain on terrace	1D chain on step
E_{Total} (eV)	1.51	0.44	0.65
E_{HB} (eV)	0.86	0.32	0.59
E_{vdW} (eV)	0.65	0.12	0.05

With the help of a simple model, one may estimate the occurrence probability to construct a linear chain formed by two kinds of molecule. Thus, consider two molecules, A and B, with an "interaction" energy such that $E_{A-A} = E_{B-B} = 1$ and $E_{A-B} = E_{B-A} = 2$, one obtains a table of the linear chain formation as described in Tab. S2. For instance, the structure in Fig. 2 is ABAABA with $n_A = 4$ and $n_B = 2$ and the corresponding energy is $E = 2 + 2 + 1 + 2 + 2 = 9$. This shows the most favourable structures for a given bicomponent chain: higher this energy number, higher the probability. For $n_A = n_B = 3$, the most favourable cases is obviously ABABAB with $E = 10$.

Table S2 Results of a simple model for the formation of a molecular chain consisting of n_A and n_B molecules (maximum of 6 molecules shown here). In each case, the number in parenthesis is the number of possible arrangements with $n_A + n_B$ molecules. The other numbers correspond to the "interaction energy" of the various arrangements with $E_{A-A} = E_{B-B} = 1$ and $E_{A-B} = E_{B-A} = 2$.

n_A / n_B	0	1	2	3	4	5	6
0	-	-	(1) 1	(1) 2	(1) 3	(1) 4	(1) 5
1	-	(1) 2	(2) 3 4	(2) 4 5	(3) 5 6 6	(3) 6 7 7	
2	(1) 1	(2) 3 4	(4) 3 5 5 6	(6) 5 6 6 7 7 8	(10) 6 6 7 7 7 8 8 8 9 9		
3	(1) 2	(2) 4 5	(6) 5 6 6 7 7 8	(10) 6 7 7 8 8 8 8 9 9 10			
4	(1) 3	(3) 5 6 6	(10) 6 6 7 7 7 8 8 8 9 9				
5	(1) 4	(3) 6 7 7					
6	(1) 5						

Molecular systems - Lander DAT ($C_{64}H_{68}N_{10}$) and Lander DCI ($C_{112}H_{102}N_2O_4$) molecules consist of a hexaphenyl benzene (HPB) core and an extended polyaromatic backbone equipped with four *tert*-butyl and 3,5-di-*tert*-butylphenyl (DTP) substituents, respectively, serving as spacer legs. The former molecule is terminated at both ends by a diamino-triazine (DAT) group while the latter is functionalized with di-carboxylic imide (DCI) groups to foster intermolecular hydrogen bonding interactions (Fig. S1a and d). Typical STM images and EHMO-ESQC calculations of the Lander DAT (Fig. S1b and c) and DCI (Fig. S1e and f) molecules show four bright lobes disposed in a rectangular shape ascribed to the tunnelling through the *tert*-butyl and DTP groups, respectively. In the case of Lander DAT molecules these bright protrusions surround a dim central part corresponding to the HPB core, while the DAT groups cannot be clearly distinguished in both STM image and calculation (Fig. S1b and c). Contrary to the case of Lander DAT, the molecular board of Lander DCI is not visualized with our experimental and theoretical tools (Fig. S1e and f).
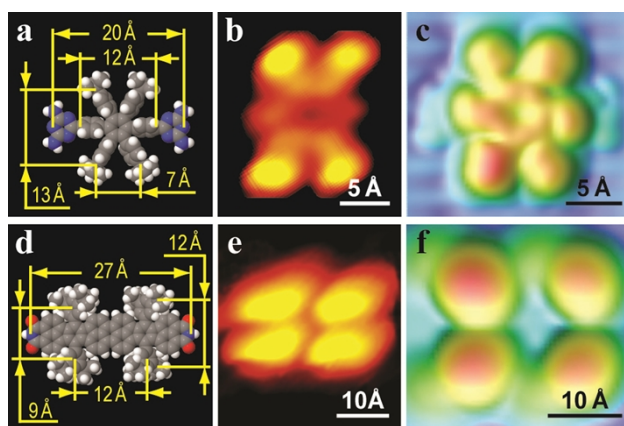

Fig. S1 (a,d) The chemical structure of Lander DAT ($C_{64}H_{68}N_{10}$) and DCI ($C_{112}H_{102}N_2O_4$), respectively. (b,e) A high-resolution STM image of a single Lander DAT ($U_T = -1.48$ V, $I_T = -0.32$ nA) and DCI ($U_T = -1.23$ V, $I_T = -0.26$ nA) on Au(111). (c,f) EHMO-ESQC calculated images of Lander DAT and DCI on Au(111) at the same tunneling conditions as in panel (b,e), respectively.

Two STM imaging modes - the formation of 2D molecular islands with grid-like structure is observed in two different STM imaging modes (Fig. S2a and b). The enhanced representations of these molecular patterns in Fig. S2c and d clearly attest that both Lander DAT (violet rectangles) and DCI (green rectangles) molecules participate in the formation of this structure. For the first imaging mode (Fig. S2c), both molecules are visualized as four lobes. Fig. S2e shows the line scans obtained perpendicular (P, P') and parallel (L, L') to the long axis of the Lander DCI and DAT molecules indicated in Fig. S2c, respectively. The distances between maxima of bright protrusions are consistent with characteristic distances of single Lander DAT and DCI molecules in Fig. S1a and d. The high brightness lobes belong to Lander DCI molecules arranged into 1D chains held together by Lander DAT molecules imaged with lower contrast. In the second STM imaging mode, the DAT molecules appear as four bright protrusions, while the DCI molecules are imaged as rods decorated by four lobes (Fig. S2d). The line scans L and P evidence Lander DCI molecules. The line scan marked B in Fig. S2d and f gives a distance of 26.5 Å in fair concordance with the backbone dimension of the Lander DCI model represented in Fig. S1d. Additionally, from this specific imaging mode one can surmise a lowering of the Lander DCI molecular board towards the surface due to attraction of the aromatic core by the metal substrate.
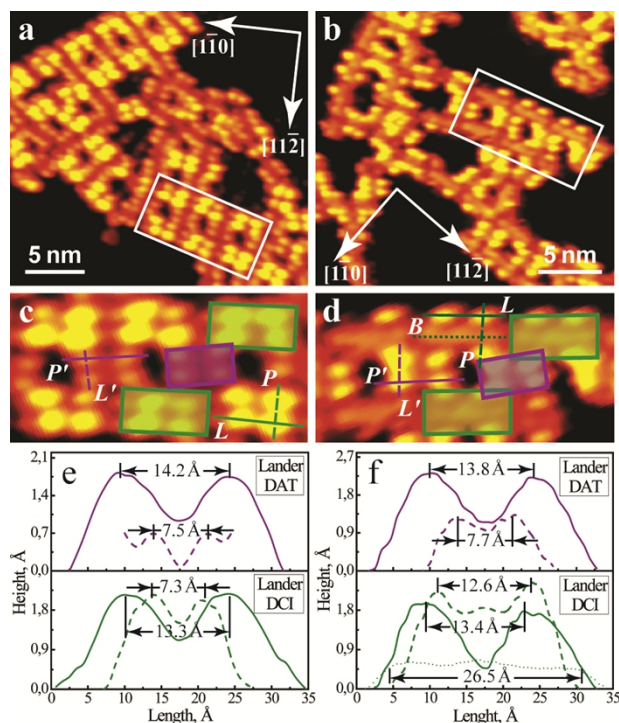

Fig. S2 (a,b) Two STM imaging modes of the 2D grid-like molecular network formed after the co-deposition of Lander DAT and DCI on the Au(111) surface, recorded at U_T = -1.25 V, and I_T = -0.51, -0.39 nA, respectively. (c,d) Enhanced representations of molecular islands in panels (a,b), where violet and green frames correspond to Lander DAT and DCI, respectively. (e,f) The line scans perpendicular and parallel to the axes of the molecules for both imaging modes.
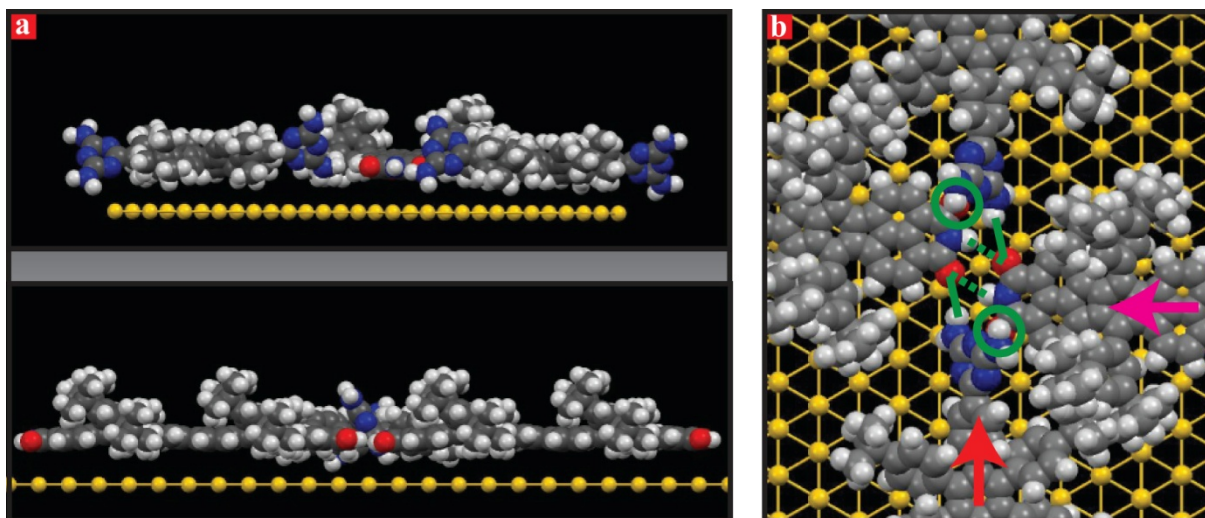
Fig. S3 Two-dimensional island formed from Lander DAT and Lander DCI on the Au(111) surface. (a) Side- and (b) top-views of the calculated model showing the H-bonding involved in formation of the 2D network. The pink and red arrows in (b) indicate the viewing directions for the side views (top and bottom panels of Fig. S3a, respectively). For clarity the DCI and DAT molecules under the arrows are removed in the side-views (top and bottom panels of Fig. S3a, respectively).
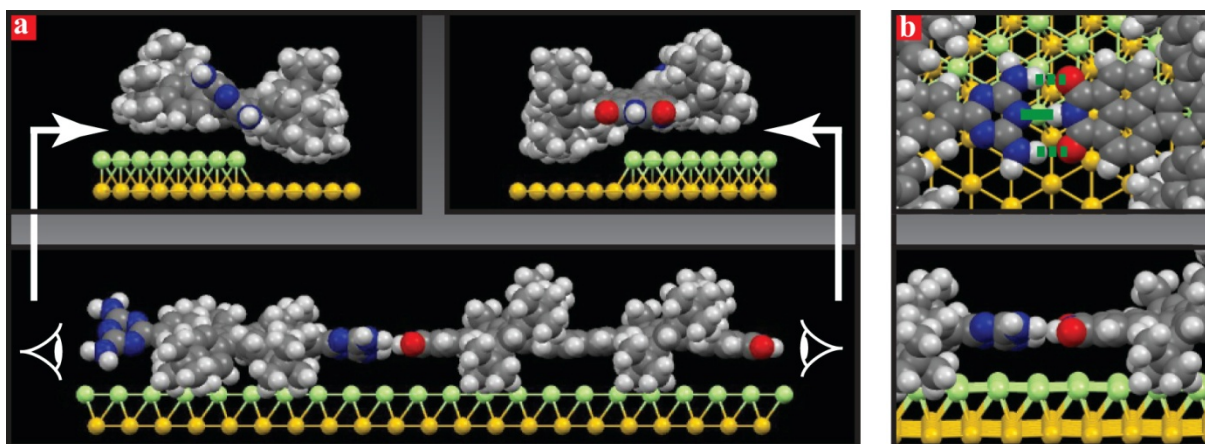

Fig. S4 Calculated conformation of the 1D chain formed from Lander DAT and Lander DCI at step edges of the Au(111) surface at step edge: (a) side view of this structure along (top panel) and perpendicular (bottom panel) to the chain, and (b) zoomed top (top panel) and side (bottom) views of the calculated model showing the H-bonding involved in formation of the 1D structure.
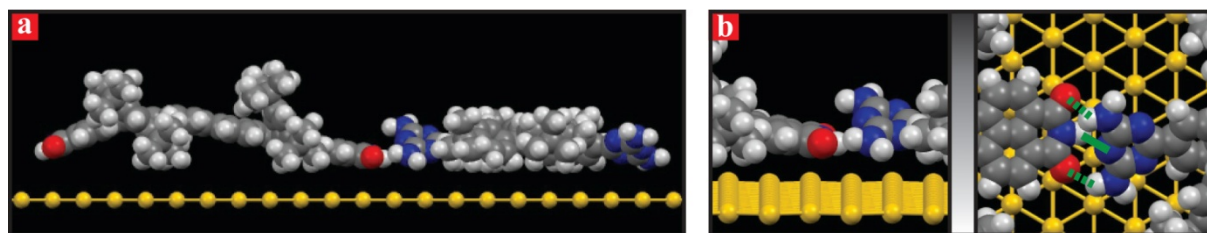
Fig. S5 Calculated model of a hypothetical 1D chain formed from Lander DAT and Lander DCI on the terrace: (a) side view and (b) zoomed side (left panel) and top views (right panel).

References

S1   P. Sautet and C. Joachim, *Phys. Rev. B*, 1988, **38**, 12238.

S2   P. Sautet and C. Joachim, *Chem. Phys. Lett.*, 1991, **185**, 23.

S3   N. L. Allinger, K. Chen and J.-H. Lii, *J. Comput. Chem.*, 1996, **17**, 642.

S4   N. L. Allinger, *J. Comput. Aided Mol. Des.*, 2011, **25**, 295.

S5   T. Zambelli, S. Goudeau, J. Lagoute, A. Gourdon, X. Bouju and S. Gauthier, *ChemPhysChem*, 2006, **7**, 1917.